International Journal of Advances in Science Engineering and Technology, ISSN(p): 2321 –8991, ISSN(e): 2321 –9009
Volume-7, Issue-4, Oct.-2019, http://iraj.in

SEMI-QUANTITATIVE ANALYSIS OF NITRIC OXIDE PRODUCTION IN THREE-DIMENSIONAL GLIOBLASTOMA MULTIFORME MODELS IN VITRO

[1]ELENA AFRIMZON, [2]YANA SHAFRAN, [3]NAOMI ZURGIL, [4]MARIA SOBOLEV, [5]MORDECHAI DEUTSCH

The Biophysical Interdisciplinary Schottenstein Center for the Research and Technology of the Cellome, Bar-Ilan University, Ramat Gan, 52900, Israel
E-mail: [1]Elena.Afrimzon@biu.ac.il, [2]yanash2000@yahoo.com, [3]zurgiln@gmail.com, [4]eweryday@yahoo.com, [5]motti.jsc@gmail.com

Abstract - Glioblastoma Multiforme (GBM) remains an incurable brain disease. One of the most important signaling molecules in the brain, nitric oxide (NO) mediates important inter- and intracellular interaction in astrocytes and neurons. In the presented study, the three-dimensional glioblastoma multicellular models were established from A-172 cells and grown in vitro in a picowell array. "Intra-spheroid" NO content and its association with mitochondrial function were studied at a resolution of single 3D object. The association between "intra-spheroid" levels of nitric oxide and mitochondrial status is revealed in real-time measurements and may serve as a significant target for tumor cure.

Keywords - Glioblastoma Multiforme, Nitric Oxide, Mitochondrial Membrane Potential, Three-Dimensional Multicellular Models in Vitro

I. INTRODUCTION

Glioblastoma Multiforme (GBM) remains an incurable brain disease. Survival rates for patients with GBM are extremely poor, with less than 5% surviving 5 years following diagnosis. Moreover, no notable improvement in population statistics has been achieved in the last three decades [1]. A better understanding of GBM pathogenesis and glioblastoma cell pathophysiology is greatly needed for development of effective treatment for this devastating disease.

One of signaling molecules that mediates important inter- and intracellular interaction in astrocytes (glioblastoma cells), is the free radical nitric oxide (NO). NO affects GBM growth, tumor cell proliferation, differentiation, and invasion ability, as well as angiogenesis, immuno- suppression, and therapeutic resistance [2], [3]. Activated glioblastoma cells produce both NO and superoxide [4]. Intracellular NO reacts rapidly with superoxide to produce peroxynitrite, which is a potent oxidant and reacts, in turn, with proteins, unsaturated fatty acids, and DNA. Also, NO radicals are produced by tumor-associated fibroblasts, activated macrophages and lymphocytes, and by endothelial cells, which are the components of tumor microenvironment which support conditions favorable to tumor progression. Moreover, glioma cells themselves, produce NO that, due to its very high diffusibility, is able to bypass the cytoplasmic membranes of neighboring cells and affect their functional activity intercellularly. Considering the significant and widespread effects of NO in both the healthy and pathological brain in general, and particularly in glioblastoma, modulation of NO levels is a feasible therapeutic strategy [2].

The complexity of tumor tissue, including cell-to-cell interaction, requires more accurate simulation of the natural three-dimensional (3D) tumor structure in vitro. Development of 3D culture models helps to bridge the gap between traditional in vitro cultures on solid substrates and complex 3D natural microenvironments in vivo. The tumor spheroid is the first in vitro model to represent a highly suitable 3D tissue-like structure elucidating inter- and intracellular signaling of cancer [5]. Spheroids maintain cell-to-cell contact, secrete extracellular matrix components, and develop active molecule transfer gradients similar to those found in physiological tissue [6]. Spheroids are an important tool in glioma research as well [7], where the structure and organization of the tissue is preserved and the microenvironmental conditions closely mimic those formed in the physiological niche [8].

Our aim is to evaluate the “intra-spheroid” NO content and its association with mitochondrial membrane potential (MMP) under activation in vitro at a single glioblastoma 3D object resolution. The association between NO production and MMP may reflect the energy capacity of 3D spheroids required for tumor cell proliferation and movement, including cell invasion capacity, and thus, tumor metastasis.

II. PROCEDURE

A. Materials

4,5-diaminofluorescein diacetate (DAF-2DA) was purchased from Calbiochem (La Jolla, CA, USA). Phorbol 12-myristate 13-acetate (PMA), Tetramethyl-rhodamine methyl ester perchlorate (TMRM), Nω-nitro-L-arginine methyl ester (L-NAME) and Glutathione Assay Kit (GSH) were

obtained from Sigma-Aldrich (St. Louis, MO, USA). NO donor Diethylenetriamine- NONOate ((Z)-1-[2-aminoethyl)-N-(2-ammonioethyl) amino] diazen-1-ium-1,2-diolate) (DETA/NO) was obtained from Alexis Biochemical (Alexis Corporation, UK). Hoechst 33342 tri-hydrochloride, trihydrate, (MW 615.99) dye was purchased from Invitrogen-Molecular probes (Carlsbad, CA, USA). DMEM, L-glutamine, sodium pyruvate, penicillin, streptomycin, FBS and trypsin were purchased from Biological Industries (Kibbutz Beit Haemek, Israel).

B. Methods

1) Glioblastoma spheroid formation and experimental procedure

Glioblastoma spheroids were established from human A-172 glioma cells. Cells were grown initially in standard conditions (37ºC, 5% CO_2 in humidified incubators) until cellular monolayer reached about 70-80% confluence. After cell detachment by trypsin, 150 µl cell suspension (final density is less than 1×10^6 cells/mL) was loaded onto a 250 µm picowell array as described previously [9] and set aside for A-172 spheroid formation over three days.

For assessment of NO generation rate, three-day A-172 spheroids were loaded on-array with a non-fluorescent cell-permeable DAF-2DA probe, which hydrolyzed within live cells by non-specific intracellular esterase, generating DAF-2. Non-fluorescent DAF-2 accumulated within the cells, are oxidized by NO, resulting in high fluorescent quantum yield. DAF-2 fluorescence intensity (FI) indicates the free NO rate within the cells. However, absolute measurement of NO concentration within the cells is quite difficult due on the one hand, to the well-known fact that NO modulates on its own synthesis, and on the other hand, that the final fluorescent product leaks with relative ease from the cells/spheroids. Thus, when the kinetics of NO content during exposure to any stimuli within spheroids is measured by FI deviation, these fluorescence measurements can only provide information on relative levels [10]. Moreover, estimation of NO kinetics under treatment at a resolution of individual 3D multicellular object reveals more precise results even in relative units (FI ratio) than averaged measurements, especially when the change in parameter values measured is small and may be undetectable in bulk measurements.

The overall mitochondrial activity in 3D multicellular A-172 spheroids was estimated by the potentiometric vital dye TMRM. TMRM FI reflects the MMP ($\Delta\psi m$) stored in the electrochemical gradient across the inner mitochondrial membrane. When TMRM accumulation is measured in individual cells, the FI standard deviation (SD) represents intracellular mitochondria vs cytoplasmic distribution of the probe [11]. On the other hand, TMRM FI across multicellular 3D spheroids recreates spatial homogeneity among all the cells. Low values of FI coefficient of variation (CV) around the mean, reflects high spheroid metabolic activity, while higher values of TMRM CV may attest to the high proportion of low-metabolic-activity cells within the spheroid [12]. As described above for DAF-2 evaluation, the change in MMP during measurement was calculated as the ratio between TMRM FI values of the first measurement in each individual spheroid and that of every subsequent image , as well as by changes in TMRM CV(%) both within the individual 3D object and the whole spheroid population.

All live fluorescent staining procedures were performed in situ while multicellular spheroids were still within the picowell array where they grow. Three-day A-172 spheroids were triple-stained with DAF-2DA, TMRM and Hoechst dyes (final concentrations 10 µM, 100 nM and 5 µg/mL, respectively) for simultaneous measurement of intracellular NO levels, MMP and total number of cells per single 3D object. After initial image acquisition, either the classic activator PMA (1 µg/mL), the NO donor DETA/NO (1 µM, 100 µM or 1000 µM) or DMSO (control) were introduced into the device in order to stimulate spheroids to produce NO. L-NAME (10 µM), L-arginine substrate-competitive inhibitor, was added on-array half an hour before activator/stimulant addition.

Early kinetic measurements were performed by imaging system over a period of 50 min from stimulant addition, while transmitted light and fluorescent images were acquired at 10 minute intervals.

2) Image Analysis and Statistics

The change in fluorescent signals within each individual 3D spheroid was measured using a motorized inverted IX81 microscope equipped with an incubator system for maintaining optimal conditions (37ºC, 5% CO_2). Spheroids were illuminated by a mercury light source. Emitted fluorescence was imaged using a CoolSNAP HQ monochrome CCD camera. Digital analysis of cellular fluorescence was performed by Olympus Cell^P software. FI values of individual spheroids were extracted using image analysis, and kinetic and end-point quantitative parameters were calculated. In order to evaluate the FI of a single spheroid, the dark current value was first subtracted from the acquired images. Then, regions of interest were defined and outlined for the bright field image separately for each spheroid and its surroundings.

Each test was performed in duplicate or triplicate. Mean and standard deviation (SD) for each measured parameter were calculated for the different spheroid populations under investigation. Comparisons between groups were performed using the t-test for groups with Gaussian distributions, and ANOVA for small groups. A paired two sample of means t-test was

used to compare two groups of cell-clusters before and after treatment. Statistical significance of differences was determined at $P < 0.05$.

III. RESULTS AND DISCUSSION

Glioblastoma 3D spheroids were established from A-172 human glioma cells within previously described 250 μm picowell array in vitro [9]. Initial cell density (0.5×10^6 cells/mL or 0.8×10^6 cells/mL) has little effect on the average number of cells initiating individual spheroid formation (37.8 ± 2.3 cells and 43.2 ± 2.2 cells, respectively, $P < 0.09$). Moreover, correlation between initial number of cells and corresponding volume of the spheroid created, have been found to decrease during spheroid growth. Correlation coefficient was calculated to be about 85% for both cell concentrations for 24 h after cell seeding and then dropped to 67% three days after cell seeding. It is believed that the main factor contributing to this effect is the cell aggregation process in the first hours after cells seeding. A-172 cells located in the single restricted picowell volume on the non-adherent surface (about 700 in each macrowell of 6-well plates) move, come into contact with each other during movement, and merge to create initial cellular clusters during the initial 24 hours (Fig. 1). These clusters become more tightly packed over the next 24h and divide into two subpopulations almost evenly (Fig. 2), one of which demonstrates diminishing spheroid volume, while the second demonstrates increasing spheroid volume. The volume ratio between 48 h and 24 h has been calculated at 0.8 ± 0.12 and 1.34 ± 0.33 in these two subpopulations ($P < 0.000001$). It's known that A-172 cell doubling time is 33h-48h [13]. In other words, two processes – cell aggregation and cell proliferation – take place simultaneously, explaining the difference between subpopulations. We can conclude that by 48 h the aggregation process is completed while 3D object growth and maturation continues. Spheroid volume has been shown to be equivalent in three-day 3D objects in both subsets ($P < 0.9$).

Three-day A-172 spheroids were triple stained (Fig. 3) on-array in situ as described in Methods, and basal NO generation rate evaluated as DAF-2 FI and MMP evaluated as TMRM FI were measured by imaging system. Although the averaged FI values of the dyes (118 ± 44.5 au for DAF-2 and 842 ± 285.2 au for TMRM) have been found to vary in individual 3D spheroids, the measured population CVs were relatively low (37% for DAF-2 and 34% for TMRM, respectively).

Due to the considerable importance of the NO molecule in healthy brain and in glioblastoma development, NO-based therapy may be a prospective strategy for treatment of GBM. Experimental modulation of intra- and extracellular NO rate can be realized by delivery of high NO concentration to the tumor cell [14] and/or by stimulation of the cells themselves to intracellular NO production resulting in cellular death.

Classic cell activator PMA was introduced to A-172 spheroids in situ, stimulating them to NO production. The immediate increase in DAF-2 FI which continues over the first 50 min after stimulator addition indicates increase of endogenous NO level (Fig. 4a). DAF-2 FI increased more than 20% in comparison to unstimulated control 3D objects (less than 10% FI increase) exposed to PMA vehicle DMSO, which was used in identical concentrations ($P < 0.001$). Distribution histograms of NO ratio values presented in Fig. 4a strongly demonstrates a significant shift in "intra-spheroid" NO level between PMA-treated and untreated spheroids. Moreover, PMA causes hyperpolarization of the MMP in the 3D A-172 spheroids (Fig. 4b). This phenomenon may be associated with the increase of endogenous NO level, but possibly to other factors as well. Treatment with NO donor, DETA/NO (Table I) shows that only very high DETA/NO concentrations resulted in MMP hyperpolarization (MHP) similar to that caused by PMA addition. Lower DETA/NO concentrations increased endogenous NO level ($P < 0.01$), but didn't influence MMP (Table I). DETA/NO decomposes spontaneously in aqueous media, releasing two 2 mol of NO per mol of parent compound. Before spheroid treatment, DETA/NO was incubated under 7.4 pH and 37ºC conditions for 1h to allow NO release [10]. As a result of DETA/NO decomposition during incubation, NO is introduced into the 3D objects in the following concentrations: 1 μM DETA/NO releases 1 nM NO; 100 μM DETA/NO releases 100 nM NO and 1000 μM DETA/NO releases 1 μM NO, respectively. Thus, the largest NO concentration, which is similar to that generated by iNOS under the various stress stimuli treatments [3], influenced both intracellular NO increase and MHP, while the lower concentration, which is similar to that produced constitutively by nNOS and eNOS [3], has no immediate or obvious effect on the mitochondrial function.

	Control	PMA	DETA/NO		
			1 μM	100 μM	1000 μM
DAF-2 ratio	1.00 ± 0.13	1.26 ± 0.27*	1.03 ± 0.02*	1.06 ± 0.04*	1.36 ± 0.2*
TMRM ratio	0.96 ± 0.11	1.11 ± 0.15*	0.92 ± 0.06*	0.95 ± 0.07	1.1 ± 0.04*

TABLE I

The endogenous rate of NO production and MMP were evaluated simultaneously under treatment with either cell activator PMA or NO donor DETA/NO, delivering the free radical extracellular in 3D

glioblastoma spheroids in vitro as described in Methods. Asterisks indicate the statistical differences in treated and untreated control 3D objects.

It was demonstrated that increased production of NO has been identified as a cause of MHP and increased mitochondrial biogenesis in T-lymphocytes. On the other hand, the key factors of cell activation pathways (like T-lymphocyte CD3/CD28 complex, Fas-Rc, or stimulation with Con A [15]) rather than endogenous NO increase exclusively, play a significant role in MMP hyperpolarization early after stimuli addition. Results presented in our study are in agreement with early reported effects of cell stimulation and may complement the information at the level of 3D multicellular objects in vitro.

In addition, previous incubation of 3D A-172 objects with concurrent L-arginine substrate L-NAME (30 min) decreased endogenous NO formation rate, while MMP was slightly increased in comparison to control untreated 3D objects (Table II). This can suggest the alternative intracellular source of NO formation which is not directly linked with NOSs activity.

TABLE II
The endogenous rate of NO production and MMP were evaluated simultaneously under treatment with cell activator PMA with or without L-NAME in 3D glioblastoma spheroids in vitro as described in Methods. Asterisks indicate statistical differences in the treated and untreated control 3D objects.

	Control	PMA	L-NAME & PMA	L-NAME
DAF-2 ratio	1.08 ± 0.14	1.26 ± 0.27*	1.02 ± 0.1*	1.02 ± 0.04*
TMRM ratio	0.98 ± 0.1	1.11 ± 0.15*	0.99 ± 0.16	1.05 ± 0.16*

Another reason for MMP increase may be associated with the change in endogenous ROS levels caused by NO/peroxynitrite pathway [4]. Indirect evidence has been found in the significant decrease ($P < 0.00004$) of intracellular reduced glutathione (GSH) FI that was revealed in spheroids incubated with L-NAME in comparison to control, and PMA-stimulated 3D objects (43.6 ± 6.5 au, 134.5 ± 38.2 au and 127.1 ± 28.7 au, respectively).

A-172 spheroids pre-incubated with L-NAME before PMA stimulation also exhibited a significant decrease in GSH FI, compared to control and PMA-stimulated objects (104.3 ± 19.9 au, $P < 0.0003$). Additionally, pre-incubation of A-172 spheroids with L-NAME, either nullifies the increase in endogenous NO levels and MMP hyperpolarization induced by PMA during the first 50 minutes, or delays these changes for more than one hour, unlike the chronic L-NAME treatment, which induces iNOS activation to generate large volumes of NO which in turn, rapidly convert to peroxynitrite [16].

IV. CONCLUSION

In the presented study, the association between "intra-spheroid" levels of NO and MMP is revealed on real-time measurements after introduction of inducer. The close interaction between these two kinetic parameters may prove to be a crucial player in glioblastoma development with potential to serve as an important target for tumor cure.

ACKNOWLEDGMENTS

This work is supported by the bequest of Moshe Shimon and Judith Weisbrodt.

REFERENCE

[1] A. F. Tamimi, and M. Juweid, "Epidemiology and Outcome of Glioblastoma," Glioblastoma [Internet] De Vleeschouwer S, editor. Brisbane (AU): Codon Publications; 2017 Sep 27. Chapter 8.

[2] P. Palumbo, G Miconi, B. Cinque, F. Lombardi**,** C. La Torre, S. R. Dehcordi, et al., "NOS2 expression in glioma cell lines and glioma primary cell cultures: correlation with neurosphere generation and SOX-2 expression," Oncotarget, 2017, 8(15): 25582-25598

[3] J. M. Fahey, and A. W. Girotti, "Nitric Oxide Antagonism to Anti-Glioblastoma Photodynamic Therapy: Mitigation by Inhibitors of Nitric Oxide Generation," Cancers 2019, 11, 231; doi:10.3390/cancers11020231.

[4] P. Manning, C. J. McNeil, J. M. Cooper, and E. W. Hillhouse, "Direct, real-time sensing of free radical production by activated human glioblastoma cells," Free Radic Biol Med. 1998 May;24(7-8):1304-9.

[5] S. Nath, and G. R. Devi, "Three-dimensional culture systems in cancer research: Focus on tumor spheroid model," Pharmacol Ther. 2016;163:94–108. doi:10.1016/j.pharmthera.2016.03. 013.

[6] T. Rodrigues, B. Kundu, J. Silva-Correia, S. C. Kundu, J. M. Oliveira, R. L. Reis, et al., "Emerging tumor spheroids technologies for 3D in vitro cancer modeling," Pharmacology and Therapeutics 184 (2018) 201–211 https://doi.org/ 10.1016/j.pharmthera. 2017.10.018.

[7] C. J. Jiglairea, N. Baeza-Kalleea, E. Denicolaïa, D. Baretsa, P. Metellusa, L. Padovania, et al., "Ex vivo cultures of glioblastoma in three-dimensional hydrogel maintain the original tumor growth behavior and are suitable for preclinical drug and radiation sensitivity screening," Exp Cell Research 2014; 321: 99 – 108.

[8] S. S. Jensen, C. Aaberg-Jessen, I. P. Jakobsen, S. K. Hermansen, S. K. Nissen, and B. W. Kristensen, "Three-Dimensional In Vitro Models in Glioma Research – Focus on Spheroids, Glioma - Exploring Its Biology and Practical Relevance," Dr. A. Ghosh (Ed.), ISBN: 978-953-307-379-8, InTech. (2011).

[9] Y. Markovitz-Bishitz, Y. Tauber, E. Afrimzon, N. Zurgil, M. Sobolev, Y. Shafran, et al., "A polymer microstructure array for the formation, culturing, and high throughput drug

screening of breast cancer spheroids," Biomaterials 31 (2010) 8436e8444.

[10] Y. Shafran, N. Zurgil, E. Afrimzon, Y. Tauber, M. Sobolev, A. Shainberg, et al., "Correlative Analyses of Nitric Oxide Generation Rates and Nitric Oxide Synthase Levels in Individual Cells Using a Modular Cell-Retaining Device," Anal. Chem. 2012, 84, 7315−7322 dx.doi.org/10.1021/ ac202741z.

[11] S. W. Perry, J. P. Norman, J. Barbieri, E. B. Brown, and H. A. Gelbard, "Mitochondrial membrane potential probes and the proton gradient: a practical usage guide," BioTechniques. 2011 Feb;50(2):98–115.

[12] Y. Shafran, N. Zurgil, M. Sobolev, E. Afrimzon, O. Ravid-Hermesh, Y. Hakuk, et al., "The role of nitric oxide in cytoprotection of breast cancer spheroids vulnerable to estrogen-induced apoptosis," Oncotarget, 2017, Vol. 8, (No. 65), pp: 108890-108911.

[13] L. N. Kiseleva, A. V. Kartashev, N. L. Vartanyan, A. A. Pinevich, and M. P. Samoilovich, "A172 and T98G Cell Lines Characteristics," ISSN 1990-519X, Cell and Tissue Biology, 2016, Vol. 10, No. 5, pp. 341–348.

[14] R. Altieri, M. Fontanella, A. Agnoletti, P. Panciani, G. Spena, E. Crobeddu, et al., "Role of nitric oxide in glioblastoma therapy: another step to resolve the terrible puzzle?," Translational Medicine 2015, 12(9): 54-59. ISSN 2239-9747.

[15] A. Perl, R. Hanczko, and E. Doherty, "Assessment of mitochondrial dysfunction in lymphocytes of patients with systemic lupus erythematosus," Methods in Molecular Biology 2012; 900: 61-89.

[16] M. D. Leo, K. Kandasamy, J. Subramani, S. K. Tandan, and D. Kumar, "Involvement of inducible nitric oxide synthase and dimethyl arginine dimethylaminohydrolase in Nω-nitro-L-arginine methyl ester (L-NAME)-induced hypertension," Cardiovasc Pathol. 2015 Jan-Feb;24(1):49-55. doi: 10.1016/j.carpath.2014.09.002**.** Epub 2014 Sep 18.

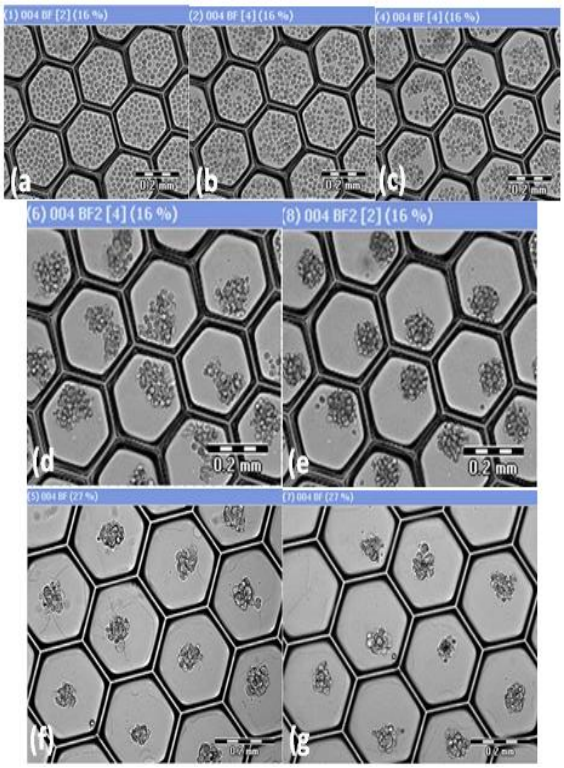

Fig. 1. The process of individual spheroid formation. A-172 cells (a) seeded in microchamber; (b) 2h 30min cell closing in; (c) 5h-7h initial cell clustering; (d) 12h-20h cell aggregation; (e) 24h cell packing; (f) 32h after seeding (note that by this time most cells in each microchamber are already arranged in one light aggregate); (g) mature spheroids at 3 days after seeding. Magnification × 20. Scale bar: 200 µm

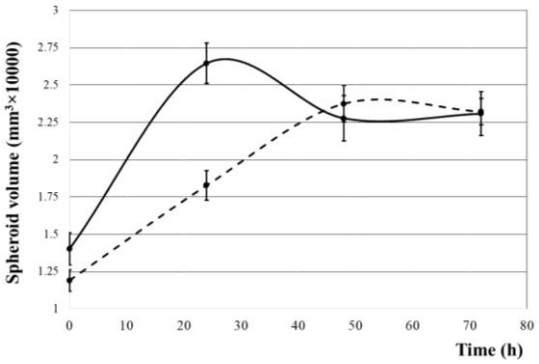

Fig. 2. Spheroid subpopulation growth

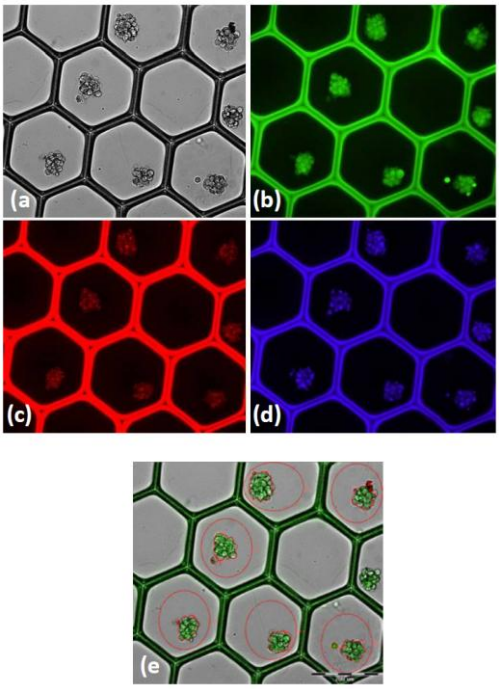

Fig. 3. Triple-staining of mature spheroids. Three-day A-172 spheroids grown within 250 µm picowell array (a), were triple-stained on-array by DAF-2DA (b), TMRM (c) and Hoechst dye (d) as described in Methods. Spheroid sample was imaged at bright field as well as at appropriate fluorescent filters. Regions of interest were defined and outlined on the BF image separately for each spheroid and for its surroundings. Overlay of the BF and corresponding fluorescent FITC images (e). Magnification × 20. Scale bar: 200 µm.

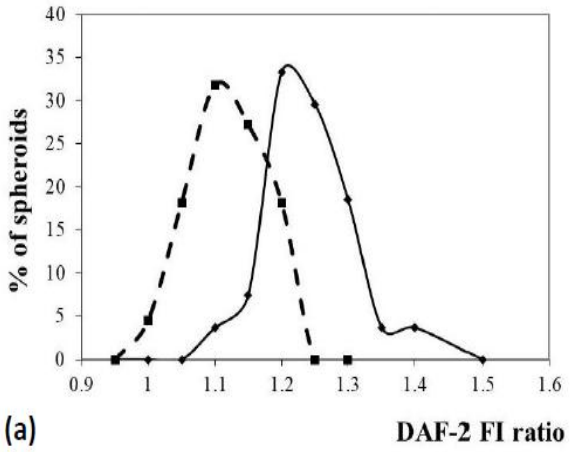

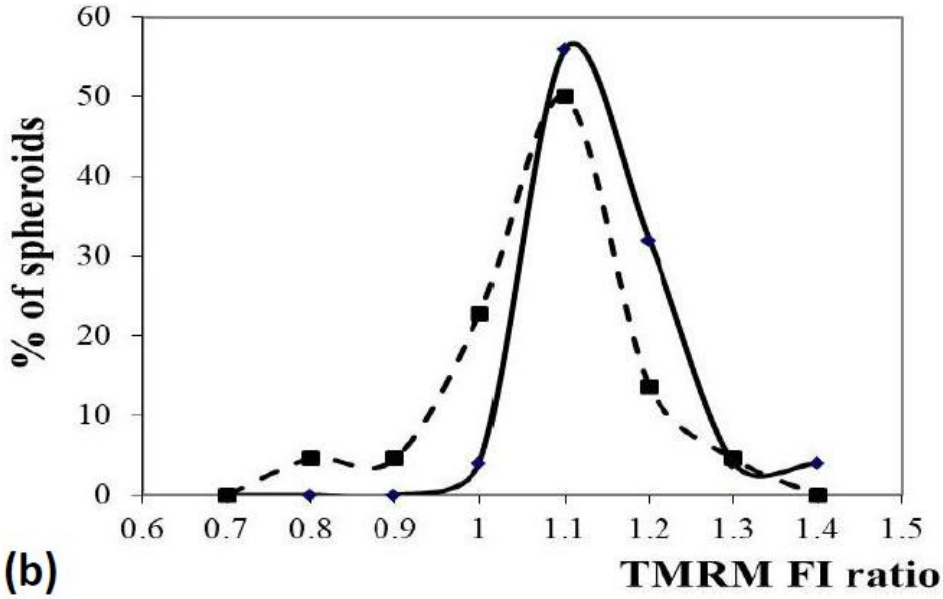

Fig. 4. Distribution histograms of DAF-2 (a) and TMRM (b) FI changes in PMA treated (solid line) and untreated control (dashed line) A-172 spheroids are presenting as FI ratios.

★★★